Evidence of Widespread Retinal Dysfunction in Patients with Stargardt Disease and Morphologically Unaffected Carrier Relatives

Susana Maia-Lopes,[1] *Eduardo D. Silva,*[1,2] *Maria Fátima Silva,*[1] *Aldina Reis,*[1,2] *Pedro Faria,*[1,2] *and Miguel Castelo-Branco*[1]

Purpose. To characterize contrast sensitivity (CS) across the visual field for two achromatic spatial–temporal frequencies in 21 families with Stargardt disease (STGD) and to correlate psychophysical impairment with patterns of change in multifocal electroretinography (mfERG).

Methods. Twenty-seven eyes from patients with STGD, 16 eyes from asymptomatic relatives, and 44 age-matched control eyes were included. Chromatic CS function was assessed by comparing protan, deutan, and tritan (Cambridge Color Test; Cambridge Research Systems Ltd., Rochester, UK) and anomaloscope measures (IF-2; Roland Consult, Wiesbaden, Germany). Achromatic CS measures were obtained with custom-made software in nine locations by using randomly interleaved staircases. The first task—low spatial frequency (LSF)—matched the known frequency-doubling method that is believed to activate the magnocellular pathway preferentially. The second included an intermediate spatial frequency (ISF, 3.5 cyc/deg). mfERGs (RETIscan; Roland Consult) were also obtained. Relatives were screened for *ABCA4* mutations by ABCR400 microarray and direct sequencing.

Results. Central impairment of achromatic and chromatic CS (along the three isolation axes) was observed in STGD. LSF and ISF tasks revealed significant and widespread dysfunction in patients and their morphologically unaffected relatives, 80% of whom were found to be *ABCA4* mutation carriers. Significant reduction of P1 amplitudes was also observed in both groups.

Conclusions. CS function is impaired in patients with STGD at distinct spatial–temporal frequencies, which, in addition to the color vision deficits, suggests dual impairment of the magnoparvocellular pathways. STGD morphologically unaffected carriers may show patterns of psychophysical dysfunction that are mirrored by abnormal mfERG responses. (*Invest Ophthalmol Vis Sci.* 2008;49:1191–1199) DOI:10.1167/iovs.07-1051

From the [1]Visual Neuroscience Laboratory, Centre for Ophthalmology, IBILI (Institute for Biomedical Research on Light and Image), Faculty of Medicine, Coimbra, Portugal; and the [2]University Hospital of Coimbra, Coimbra, Portugal.

Supported by Grant POCI_SAU-OBS_57070-2004, Fundação para a Ciência e Tecnologia (FCT, Portugal), a grant from the Gulbenkian Foundation on Retinal and Brain Degenerations, and funds from the EVI-GENORET European Network. SM-L and MFS were supported by individual FCT fellowships POCI/FSE: SFRH/BD/11828/2003 and SFRH/BD/18777/2004.

Submitted for publication August 12, 2007; revised October 18 and November 16, 2007; accepted January 23, 2008.

Disclosure: **S. Maia-Lopes**, None; **E.D. Silva**, None; **M.F. Silva**, None; **A. Reis**, None; **P. Faria**, None; **M. Castelo-Branco**, None

The publication costs of this article were defrayed in part by page charge payment. This article must therefore be marked "*advertisement*" in accordance with 18 U.S.C. §1734 solely to indicate this fact.

Corresponding author: Miguel Castelo-Branco, Centre for Ophthalmology, IBILI, Faculty of Medicine, Az. de Sta Comba, 3000–354 Coimbra, Portugal; mcbranco@ibili.uc.pt.

Stargardt macular dystrophy (STGD; OMIM 248200; http://www.ncbi.nlm.nih.gov/Omim/ Online Mendelian Inheritance in Man; National Institutes of Health, Bethesda, MD),[1] accounts for 7% of all retinal dystrophies and affects approximately 1 in 10,000 people, with a typical onset during childhood and a predominantly autosomal recessive inheritance[1–5] Bilateral retinal atrophic lesions may have a "beaten-metal" appearance, and the pattern of distribution, number, and shape of the flecks is variable and can change over time.[4–7] Accumulation of lipofuscin-like material in the retinal pigment epithelial (RPE) cells is thought to be the cause of diffuse blockage of choroidal filling on fluorescein angiography ("choroidal silence"), which often occurs in these patients.[8–10]

In 1993, Kaplan et al.[2] mapped the locus for STGD/FFM (fundus flavimaculatus) to the short arm of chromosome 1 and *ABCA4*, a photoreceptor-specific adenosine triphosphate (ATP)-binding cassette transporter, was subsequently characterized. Several groups performed mutation analysis of *ABCA4* in STGD/FFM patients, and more than 490 sequence variations have recently been identified.[11–13] Such high allelic heterogeneity within the 50 exons of *ABCA4* makes it difficult to predict the disease-causing variants. It is likely that the wide variation in retinal phenotype within families (age of onset, disease severity, pattern of lipofuscin accumulation, ERG results, visual acuity) may be explained by different combinations of *ABCA4* mutations segregating within a single family[5–8,14] Furthermore, mutations in this gene have also been implicated in other macular dystrophies.[15–18]

Given that STGD-FFM involves symptoms mostly related to cone dysfunction, it was surprising that first reports of *ABCA4* expression found its presence in rod but not in cone photoreceptors.[19] However, later, it was shown by immunofluorescence microscopy and Western blot analysis that *ABCA4* is expressed in foveal and peripheral cones and in rod photoreceptors.[20] In accordance with *ABCA4* expression in cones and with the main clinical manifestations, Scholl et al.[21] found that long (L) and M (middle)-wavelength cone driven ERGs exhibit phase and amplitude alterations in STGD.

The main intent of the present study was to establish topographical characterization of psychophysical performance in patients with STGD and their morphologically unaffected relatives, in which concerns contrast sensitivity within distinct spatial frequency channels. We further sought to establish the phenotyping value of this strategy in members of families with STGD and their correlation with multifocal electrophysiological (mfERG) measures. We have also quantified L-, M- and S-cone function using a psychophysical method that has already been shown to be useful in understanding structure–function correlations in other macular dystrophies, namely Best disease.[22] Of importance, we have used the above-mentioned methods to study clinically and genetically characterized asymptomatic relatives, as revealed by normal ophthalmic examination. The goal was to test the possibility of subtle visual impairment in putative carriers, whose carrier state was assessed.

TABLE 1. Clinical Characteristics of Patients with Stargardt Disease and Their Relatives

Family	Subjects	Sex	Phenotype	CFC	Age (y)	Onset (y)	Duration (y)	VA		Color Vision
								OD	OS	
1	CAP	M	Stargardt	Severe	42	7	35	1/10	1/10	P+T
	PCP	M	Stargardt	Severe	38	14	24	1/10	0.5/10	D+T
	ELP	M	Stargardt	Severe	33	11	22	1/10	1/10	P+T
	ARP	M	Relative (father)	No changes	66	—	—	10/10	10/10	Normal
2	ACO	F	Stargardt	Mild	8	5	3	8/10	6/10	Normal
	TMO	M	Stargardt	Severe	12	8	4	1/10	8/10	T
	CAO	F	Relative (sister)	Subtle*	8	—	—	10/10	10/10	Normal
3	DMB	M	Stargardt	Moderate	16	6	10	1.6/10	1.6/10	P
	GMB	M	Relative (brother)	No changes	19	—	—	10/10	10/10	Normal
4	MJG	M	Stargardt	Severe	34	6	28	FC	FC	NP
	MAS	F	Relative (sister)	No changes	36	—	—	10/10	10/10	Normal
5	MRA	F	Stargardt	Severe	17	12	5	1/10	1/10	P+T
	MCA	F	Relative (mother)	No changes	40	—	—	10/10	10/10	Normal
6	MCB	F	Stargardt	Moderate	20	14	6	1/10	1/10	P
	LCB	M	Relative (brother)	No changes	30	—	—	10/10	10/10	D
7	RCG	M	Stargardt	Moderate	24	11	13	0.5/10	0.5/10	P+T
	VCG	F	Relative (sister)	No changes	17	—	—	10/10	10/10	P
8	RMF	M	Stargardt	Moderate	11	9	2	0.5/10	1/10	P+T
	JMF	M	Relative (brother)	No changes	18	—	—	10/10	10/10	Normal
9	RFF	M	Stargardt	Moderate	9	7	2	0.5/10	1/10	Normal
	DRN	F	Relative (mother)	No changes	36	—	—	10/10	10/10	P
10	MCR	M	Stargardt	Moderate	27	24	3	1.2/10	1.2/10	P+T
	SCR	F	Relative (sister)	No changes	23	—	—	10/10	10/10	T
11	JGK	M	Stargardt	Severe	29	9	20	FC	FC	NP
	AGK	F	Relative (sister)	No changes	31	—	—	10/10	10/10	T
12	LMO	M	Stargardt	Moderate	43	43	0	1/10	3/10	NP
13	CAO	M	Stargardt	Moderate	61	30	31	0.5/10	0.5/10	T
	MGO	M	Stargardt	Moderate	40	30	10	6/10	8/10	P
	JLO	M	Relative (brother)	Subtle*	54	—	—	10/10	10/10	P+T
14	PRL	F	Stargardt	Severe	11	7	4	1/10	1/10	P+T
	POL	F	Stargardt	Severe	11	7	4	1/10	1/10	P+T
	GBR	M	Relative (father)	No changes	39	—	—	8/10	6/10	Normal
15	PGP	F	Stargardt	Moderate	14	9	5	1/10	1/10	NP
16	ACA	F	Stargardt	Moderate	32	27	5	1/10	1/10	P+T
17	JGF	M	Stargardt	Moderate	30	29	1	2.5/10	1.6/10	D+T
	CGF	M	Stargardt	Moderate	25	25	0	3/10	FC	P+T
18	JMD	M	Stargardt	Mild	10	9	1	2/10	2/10	T
	CMD	F	Relative (sister)	No changes	8	—	—	10/10	10/10	Normal
19	ZMC	F	Stargardt	Moderate	25	17	8	2/10	2/10	D
20	TCC	M	Stargardt	Mild	7	1	6	1/10	1/10	P+D+T
	MLC	F	Relative (mother)	No changes	34	—	—	10/10	10/10	Normal
21	CRG	M	Stargardt	Mild	16	9	7	0.5/10	2/10	T
	BRG	F	Relative (sister)	No changes	11	—	—	10/10	10/10	Normal

Data include gender, phenotype, central fundus changes (CFC), age at examination, age of onset, duration of disease, VA of the right (OD) and left (OS) eyes, and color vision (CV) results from anomaloscope testing. CFC: mild = normal to diffuse foveal reflex, subtle pigment mottling of the macular RPE, tapetal sheen or beaten-metal reflex; moderate = pronounced hyper- and hypopigmentation of the macular RPE, bull's-eye atrophy; severe = widespread confluent areas of RPE and/or choroidal atrophy; FC, visual acuity reduced to finger counting; P, protanomalous; D, deuteranomalous; T, tritanomalous; NP, the subject could not perform the test.

* Siblings CAO and JLO had subtle changes in the fundus that did not fulfill the criteria for Stargardt disease.

METHODS

Characterization of the Clinical Group

Twenty seven patients with Stargardt (n = 27 eyes; mean age: 23.9 ± 13.5 [SD] years, range: 7–61) and 16 morphologically unaffected relatives with normal ophthalmic examination findings (n = 16 eyes; mean age: 29.3 ± 16.2 years, range: 8–66) from 21 families were included in the study and compared with an age-matched group of 22 normal control subjects (n = 44 eyes, mean age: 28.0 ± 15.9 years, range: 6–69 years). Analysis of variance showed no significant age difference between groups (F test; P = 0.118 for normal versus relatives, P = 0.534 for normal versus STGD group, and P = 0.385 for relatives versus STGD group).

The clinical ophthalmic examination performed in all participants included best-corrected visual acuity (VA) obtained by postcycloplegic manifest refraction on Snellen charts, slit-lamp examination, fluorescein angiography and dilated fundus examination by direct and indirect ophthalmoscopy. We staged our patients according to the criteria for increasing severity described by Scholl et al.[21] Only subjects presenting no other eye diseases were included. The age of onset was defined as the age at which decreased VA was first noted. Clinical data of patients with STGD are shown in Table 1.

Informed consent was obtained from all subjects after explanation of the objectives and possible consequences of the study, in strict accordance with the institutional guidelines defined by the ethics committee of the Faculty of Medicine of Coimbra. The research was conducted in accordance with the tenets of the Declaration of Helsinki.

Psychophysics

Color Psychophysical Tasks. All subjects underwent color vision testing both for the Rayleigh or Moreland equations by

means of a anomaloscope (IF-2; Roland Consult, Wiesbaden, Germany; Table 1).

Whenever possible, patients ($n = 9$) were also tested for the three main cone-confusion axes, simultaneously and in an interleaved manner,[22] by modulating chromaticity in CIE 1976 u′v′ color space, using a slightly modified version of the Cambridge Color Test (Cambridge Research Systems Ltd. [CRS], Rochester, UK). Subjects looked monocularly at a screen with a pattern of disks of various sizes and luminance with superimposed chromatic contrast defining a Landolt-like C-shaped ring. Subjects performed this test monocularly with the better eye and were instructed to indicate the gap position, whereas the chromaticity of the Landolt C was adjusted according to the staircase procedure. Psychophysical thresholds were assessed simultaneously through three parallel randomly interleaved staircases.[23,24] Maximum and minimum excursion were 0.11 and 0.002 units in u′v′ color space, respectively. Each staircase was composed of 11 reversals, and the mean of the last 7 reversals was taken as the threshold estimate. Viewing distance was 56 cm, and the Landolt-like C-shaped ring had the following dimensions: gap size, 5.14°; outer diameter, 24.43°; and inner diameter, 12.25°.

CS Achromatic Psychophysical Tasks. CS was assessed independently for each location (up to 20° of the visual field) in a randomly interleaved manner, with several staircases running in parallel at each position.

Two different types of vertically oriented sinusoidal gratings were used: LSF, 0.25 cycles per degree (cyc/deg) grating stimuli, flickering at 25 Hz, mimicking the frequency-doubling method, to characterize magnocellular function[25,26]; and ISF, 3.5 cyc/deg static stimuli. Grating stimuli were generated from a graphics card (CRS/VSG 2/5; CRS) and displayed on a gamma-corrected 21-in. color monitor (frame rate 100 Hz; Trinitron GDM-F520; Sony, Tokyo, Japan) at a viewing distance of 36 cm. Mean background luminance was 61.7 and 51 cd/m^2 for LSF and ISF conditions, respectively.

Luminance modulation of the stimulus was expressed according to Michelson luminance contrast (%) = $100 \cdot (L_{max} - L_{min})/(L_{max} + L_{min})$. Staircases were implemented by means of an adaptive logarithmic strategy and were run for a total of four reversals, with the contrast of the last two reversals being averaged to estimate contrast threshold. The results were expressed in decibels units, dB = $20 \cdot \log (1/c)$, with contrast (c) measured as a percentage.

This perimetric test was performed monocularly on the better eye. The subjects were instructed to fixate a black square (1° × 1°) in the center of the screen and report the presence of vertical "striped" targets (detection task) by means of a button press. Stimulus duration was 200 ms, and ISI (interstimulus interval) was jittered between 2300 and 2800 seconds. Participants' reliability was evaluated by the inclusion of false-positive and -negative "catch trials," and all results with false-positive and -negative errors ≥ 33% were excluded, according to standard criteria.[27] Fixation loss was monitored by means of eye-tracking methodology (infrared CRS monitoring device).

For the analyses of CS eccentricity dependence, three zones were defined: zone 0, the 5° central region; zone 1 comprises locations at 5° to 10° eccentricity; and zone 2 corresponds to locations at 10° and 20° eccentricity (for details, see Fig. 3A).

Electrophysiological Recordings

We recorded mfERG by using DTL fiber electrodes, after 10 minutes of light adaptation and pupil dilation with tropicamide (RETIscan System; Roland Consult). Pupil diameter after dilation was, on average, ~7 mm. The stimulus consisted of 61 hexagons, covering ~30° of visual field and presented on a 20-in. monitor at a viewing distance of 33 cm. Refractive errors were corrected for the viewing distance. The hexagon areas increased with eccentricity to compensate differences in cone density across the retina (leading to a fourfold size change). Each hexagon was temporally modulated between light and dark (frame rate: 60 Hz; maximum luminance: ~120 cd · m^{-2}). Observers were instructed to fixate a small black cross in the center of the stimulus. Fixation was checked by means of online video-monitoring during the ~8 minutes lasting recording sessions and high-amplitude artifacts were automatically eliminated. Data for three of the patients with STGD were excluded from the statistical analysis, either because of their very low signal-to-noise responses or unstable fixation. To improve fixation stability, sessions were broken into 47-second segments, and eight trials were recorded in total. Signals were amplified with a gain of 100.000 and band-pass filtered (5–300 Hz). The surface electrode impedance was less than 10 kΩ. First-order kernels were analyzed because of their closer correlation with the function of the outer retina and to avoid temporal adaptation mechanisms that are generally considered to influence higher-order kernel analyses.[28] The local responses obtained were divided by the respective stimulus area to obtain the density-normalized response (nV/deg^2). For each hexagon, the amplitude of P1 (defined as the difference between N1 and P1 components) was calculated, and the implicit time of the P1 component determined. To evaluate eccentricity dependence between group differences of the local ERG responses, we obtained averaged responses across five concentric rings around the fovea.

ABCA4 Gene Mutation Detection

Relatives were screened for variants of the 50 exons of the *ABCA4* gene by means of the ABCR400 microarray, according to a procedure described by Jaakson et al.[29] All genotyping results were confirmed by direct sequencing. The exons in which their affected STGD family member(s) were found to have any mutation were further sequenced.

Genomic DNA was extracted from peripheral blood samples with an automated DNA extractor (BioRobot EZ1; Qiagen, Valencia, CA). The primers were as described elsewhere.[30] Sequencing reactions were performed with a four-dye terminator cycle sequencing ready-reaction kit (BigDye Terminator ver. 1.1, Applied Biosystems, Inc. [ABI], Foster City, CA), and the sequence products were purified and resolved (Prism 3130; ABI).

Statistical Analysis

We performed analysis of variance (ANOVA), with the post hoc Fisher PLSD (protected least-significant difference) correction, using statistical software (Statview; SAS, Cary, NC). Results with $P < 0.05$ were considered statistically significant. Correlation analyses were performed with Fisher-to-Z transformation of Pearson coefficients.

Results

Patterns of central fundus changes, age of onset, disease duration, VA of the right and left eyes, and patterns of color vision impairment as assessed by the anomaloscope are indicated in Table 1. Central fundus changes were, in general, symmetric across the patients' eyes. In 5 (24%) of 21 families studied, more than one sibling was affected. In these families, the intrafamilial variability in age of onset was reduced, with a maximum mean deviation of 2.4 years (average mean deviation, 1.2 years). The pattern of central fundus alterations in patients belonging to the same family was also very similar, even when the estimated severity was not the same (Fig. 1).

Psychophysics

Color Psychophysical Tasks. Twenty-one patients with STGD were tested with the anomaloscope, and only two were found to have normal color vision. Tritan (76%) and protan (62%) were the color anomalies more often found in our patients, whereas deutan anomalies were less frequent (19%). Alterations in more than one of the colorimetric equations (Rayleigh and Moreland) were often detected (13/27 patients). On the other hand, when we attempted quantitative characterization of relative damage of each cone population through a slightly modified version of Cambridge Color Test (CCT; CRS), nine patients (who were not acuity limited for this

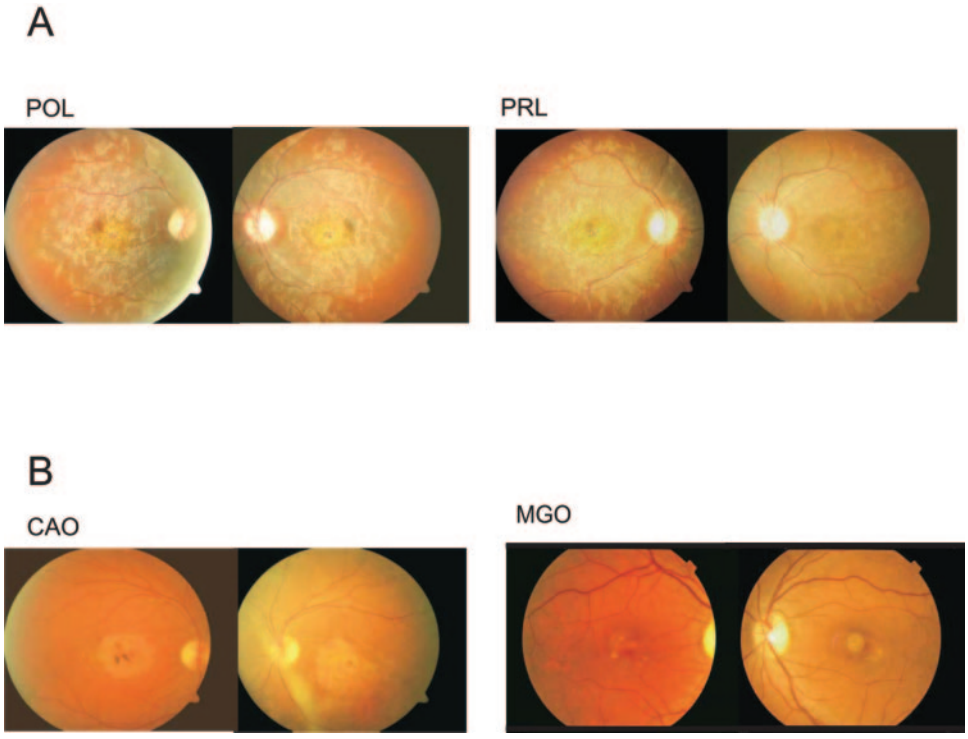

FIGURE 1. Typical intrafamilial patterns of variability of central fundus changes in STGD families. (**A**) Siblings belonging to family 14 with more similar fundus changes are shown. (**B**) Siblings from family 13 with moderate central fundus changes and a distinct pattern.

specific test), with mean disease duration of 8.2 ± 3.1 years (VA: 0.1–0.8), were included. As shown in Figure 2, statistically significant impairment of all three cone channels was observed in patients with STGD ($P < 0.0001$ for protan, deutan, and tritan axes; Fisher PLSD). However, in patients with shorter disease evolution, more evident damage in protan and deutan axes was found (protan: from mean 45.4×10^{-4} u′v′ units in control subjects to 350.0×10^{-4} in patients, $P < 0.0001$; deutan: from 44.8×10^{-4} u′v′ units in the normal group to 409.1×10^{-4} u′v′ in patients with STGD, $P < 0.0001$; tritan: 63.5×10^{-4} u′v′ units in control subjects to 185.2×10^{-4} in patients, $P < 0.0001$). No significant relation was observed between disease stage and color vision deficiencies. Relatives of patients with STGD were not significantly impaired in this task, except for the tritan axis (103.6×10^{-4} u′v′ units, $P = 0.003$).

CS Achromatic Psychophysical Tasks. Representative maps of CS obtained for the two stimuli conditions (LSF and ISF) from representative (close to the median) patients with STGD, morphologically unaffected relatives, and control subjects are shown in Figures 3 and 4. As expected from known relative cone distributions, CS was higher in central locations than in the more peripheral regions for both CS methods. The LSF task yielded higher CS than did the ISF-task in all groups (in age-matched control subjects mean CS was 29.4 ± 3.4 dB in the LSF-condition and 25.2 ± 7.2 dB in the ISF perimetric tests). Three patients with STGD were excluded (of 27) due to unstable fixation.

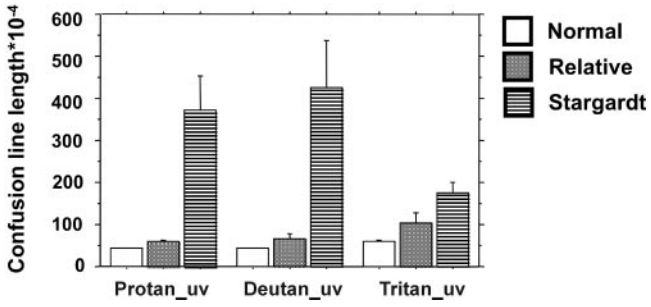

FIGURE 2. Mean length of chromatic discrimination vectors (protan, deutan, and tritan) were significantly increased in patients with STGD, but the effect did not reach significance in STGD relatives, except for the tritan axis (103.6×10^{-4} u′v′ units; $P = 0.003$).

LSF-biased perimetry revealed significant impairment in patients with STGD in comparison to their relatives and control subjects ($P < 0.0001$ for both comparisons). Of note, the patients' performance was significantly impaired across the whole visual field and not only at the central-most regions ($P < 0.0001$ for zones 0, 1 and 2, for both CS methods). For the ISF task the deterioration of CS function in patients with STGD was even more evident (patients' mean CS was 17.3 ± 8.7 and 10.8 ± 7.7 dB for the LSF and ISF tasks, respectively).

Concerning morphologically unaffected relatives, LSF perimetry showed, as expected, significantly better performance than in patients with STGD for all tested zones ($P = 0.0008$ for zone 0; $P < 0.0001$ for zones 1, 2). However, we were surprised to find significant differences between these morphologically unaffected relatives and control subjects across the whole visual field ($P < 0.0013$, $P = 0.0045$, and $P = 0.0009$, for zones 0, 1 and 2, respectively). Again, similar results were obtained with the ISF test ($P < 0.0187$, $P < 0.0001$, and $P = 0.0012$ for zones 0, 1, and 2, respectively). These asymptomatic relatives had CS performances that were between the patients with STGD and the control group, for both CS tasks (mean CS was 26.5 ± 5.3 and 21.0 ± 8.2 dB for the LSF and ISF conditions, respectively). In summary, STGD relatives seem to be relatively impaired in both CS tasks. In other words, morphologically unaffected relatives might represent a pre-STGD stage with CS impairment (also discussed later in the article).

Electrophysiological Recordings

Examples of mfERGs obtained from representative patients with STGD, STGD morphologically unaffected relatives, and age-matched control subjects are shown in Figure 5A.

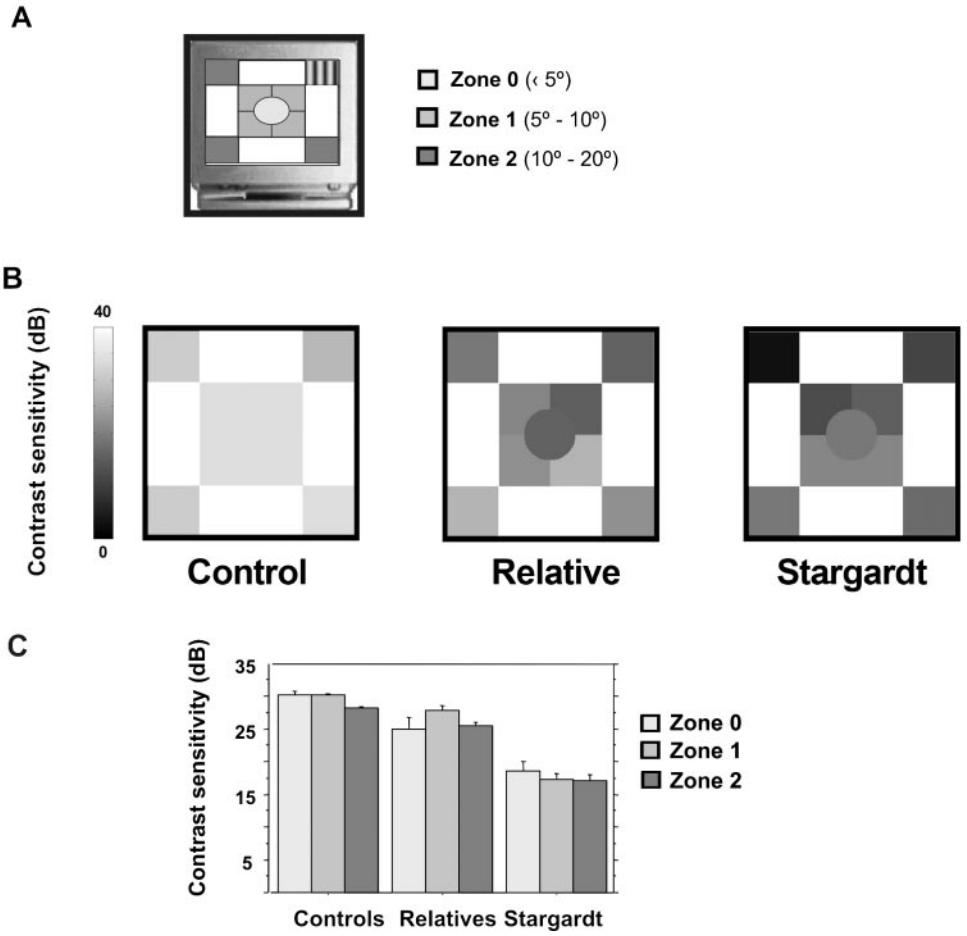

FIGURE 3. CS in Stargardt families obtained by the LSF testing method. (**A**) Stimulus display for both CS tests. (**B**) Maps of CS from representative individuals from the STGD group, STGD relatives, and control group. (**C**) CS at three zones of increasing eccentricity obtained in the three groups. Impairment of CS function was evident in patients with STGD at all eccentricities. Surprisingly, STGD relatives were also found to be impaired in this LSF-CS task.

By comparison with relatives and age-matched control subjects, patients with STGD showed significant smaller P1 amplitudes, with the typical loss of the central retina peak ($P < 0.0001$ for both comparisons to relatives and control subjects). This amplitude reduction was strong and very significant for all the eccentricity rings ($P < 0.0001$ for all rings 1–5).

Of note, STGD morphologically unaffected relatives showed further evidence for some degree of physiological impairment, with P1 amplitudes significantly larger than patients and significantly smaller than control subjects. P1 amplitudes in STGD relatives were significantly decreased in the more central rings but not in the more peripheral ones compared with age-matched control subjects ($P = 0.0043$, $P = 0.0016$, and $P = 0.008$ for rings 1, 2 and 3, respectively; NS for rings 4 and 5).

Implicit times of the P1 component were analyzed for all eccentricities. We observed that mfERG responses from patients with STGD were significantly delayed in the more eccentric rings compared with those of unaffected relatives and control subjects (rings 3: $P < 0.02$ and $P = 0.0035$ for comparisons to relatives and control subjects; rings 4, 5: $P < 0.0001$ for both comparisons). No significantly delayed responses were observed in the group of STGD relatives.

Correlations between Psychophysics, Electrophysiology, and Disease Progression

To evaluate whether psychophysical and electrophysiological measurements conveyed independent information, we performed correlation analyses (with Fisher-to-*Z* transformation) between LSF- and ISF-CS measures and P1 amplitudes. Correlation analyses between corresponding areas revealed significant correlations within 5° to 20° zones for the LSF but not for the ISF sensitivity measures (correlation coefficient [cc] = 0.477 and $P = 0.03$ for 5° to 10°, cc = 0.431 and $P = 0.057$ for 10° to 20° locations for LSF-task). To improve the statistical power, we then correlated global CS performance obtained in both LSF- and ISF- methods with P1 summed-amplitude responses and found significant correlations (LSF task: cc = 0.517 and $P = 0.018$; ISF-task: cc = 0.481 and $P = 0.043$), suggesting global level correlations between psychophysical and electrophysiological responses and at least a partially common neural substrate.

No significant relation was observed between disease stage and color vision deficiencies. However, performance in LSF, ISF-CS tasks and P1 amplitude responses correlated highly with disease stage, as revealed by ANOVA. Of interest, P1 amplitude and LSF-CS were significantly impaired in the "moderate" disease stage compared with the "mild" stage ($P = 0.0033$ for P1 amplitude and $P = 0.0059$ for the LSF-CS task); however, a further progressive deterioration to the "severe" stage was only significant for CS tasks ($P < 0.0001$ for both ISF- and LSF-CS methods). These results extend the notion of progressive CS impairment across stages once STGD is established. None of the phenotypical methods applied showed any correlation with disease duration, as indexed by the onset of decay in VA.

Genetic Characterization

In this study, we investigated *ABCA4* mutations in asymptomatic relatives, where 12 (80%) of 15 subjects studied were found to be carriers (Table 2). Twelve different putatively disease-causing alterations were identified, including nine missense amino acid substitutions (75%), two frameshifts (16.7%),

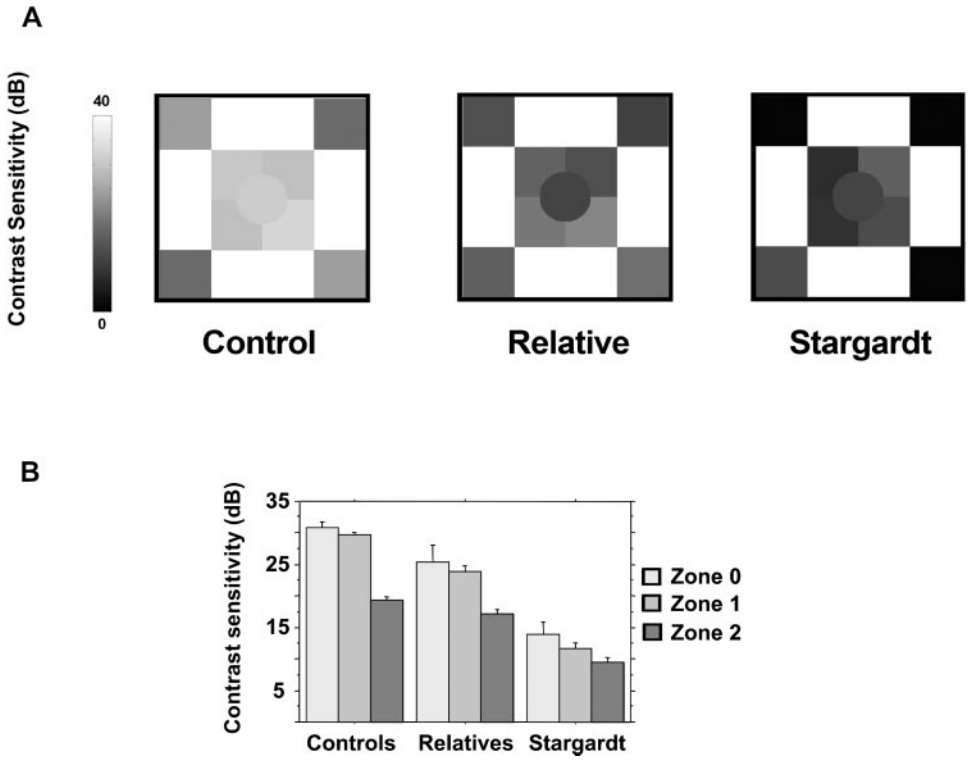

FIGURE 4. CSF in subjects from STGD families obtained by the ISF testing method. (**A**) Maps of CS obtained from representative individuals from each group. (**B**) CS at three zones of eccentricity obtained from the three groups. Again, severe impairment in CS function was observed in patients with STGD at all eccentricities. STGD relatives were again found to be impaired in this achromatic CS task.

and one splicing variant (8.3%). The most frequent mutation found was the missense variant G1961E (6.7%) that, even in the heterozygous state, has been significantly associated with age-related macular degeneration (AMD).[16] One missense mutation involving an uncharged amino acid (L11P) in a conserved domain that has been found in FFM patients was detected. Several other sequence changes that have been significantly correlated to the STGD phenotype (M1V, N96D, R290W, L2027F, R2030Q, V2050L, 3211insGT, and IVS40+5G>A) were also identified. Furthermore, two mutations were found for the first time (M1T, 4034delAC) and were not present in 102 control chromosomes but in their respective STGD-affected members. Both novel mutations may induce a severe phenotype, since similar variations in the same codons (missense M1V and insertion 4035insCA) are thought to be STGD and CRD associated, respectively. Overall, five mutations may be interpreted as null: the missense changes affecting the initiation codon (M1V and M1T), two frameshift alterations (3211insGT, 4034delAC), and one splice variant (IVS40+5G>A). Only one subject (MCA) was found to carry a complex allele. No *ABCA4* mutation was detected in 6 (20%) of 30 studied alleles from relatives belonging to three STGD families. Nevertheless, in two of these families, no *ABCA4* mutation was identified in the affected family member.

In the case of subject CMD, relative with the homozygous wild-type genotype, we confirmed the absence of the two mutations detected in her affected sibling. As expected, we observed in this case a relatively high performance in all psychophysical tasks and robust physiological responses. (She was at the 90 percentile for both psychophysical and electrophysiological measures, which was the expected result for this negative control.) In addition, to exclude the possibility that peripherin*/RDS* gene mutations were involved in such STGD families with no *ABCA4* mutation identified, we assessed mutation analyses of the former gene by direct sequencing of those families, and again no causal sequence change was identified (data not shown).

DISCUSSION

We have provided a topographic characterization of visual impairment, using psychophysical and electrophysiological approaches, in patients with STGD, their morphologically unaffected relatives, and unrelated control subjects. To our knowledge, this is the first report describing physiological impairment in STGD relatives with an apparently normal phenotype, as documented by a gold-standard ophthalmic examination, in which the *ABCA4* mutation carrier state was assessed. A recent study on multifocal pattern dystrophy simulating STGD showed that asymptomatic family members could show development of discrete retinal abnormalities. However, in this previous report, an autosomal dominant inheritance pattern was identified, and mutations in peripherin/*RDS* were causal,[31] which was not the case in our study.

With our custom-made CS methods, we were able to show that patients with STGD are dramatically impaired in their sensitivity up to 20° of the visual field. The amount of CS loss shown by patients with STGD was greatest at the highest tested stimulus spatial frequency. Furthermore the most dramatic impairment was observed at eccentric locations for the ISF task compared with the LSF condition. This finding of different CS profiles across tests also suggests that the two distinct types of gratings used show a different activation bias concerning parvo- and magnocellular visual pathways.[32,33] LSF gratings flickering at 25 Hz favor the activation of magnocellular pathway, which is consistent with the higher CS that was obtained with such stimuli. This finding is in accordance with electrophysiological measures in primates, and this argument has been used to justify its application in patients with glaucoma to evaluate magnocellular damage.[34–37] We speculate that the ISF condition may better stimulate the parvocellular visual pathway (at least compared with the more magno-like LSF condition). Accordingly, the lower observed CS could reflect the lower photoreceptor-bipolar-ganglion cell convergence within the parvocellular pathway.[38,39]

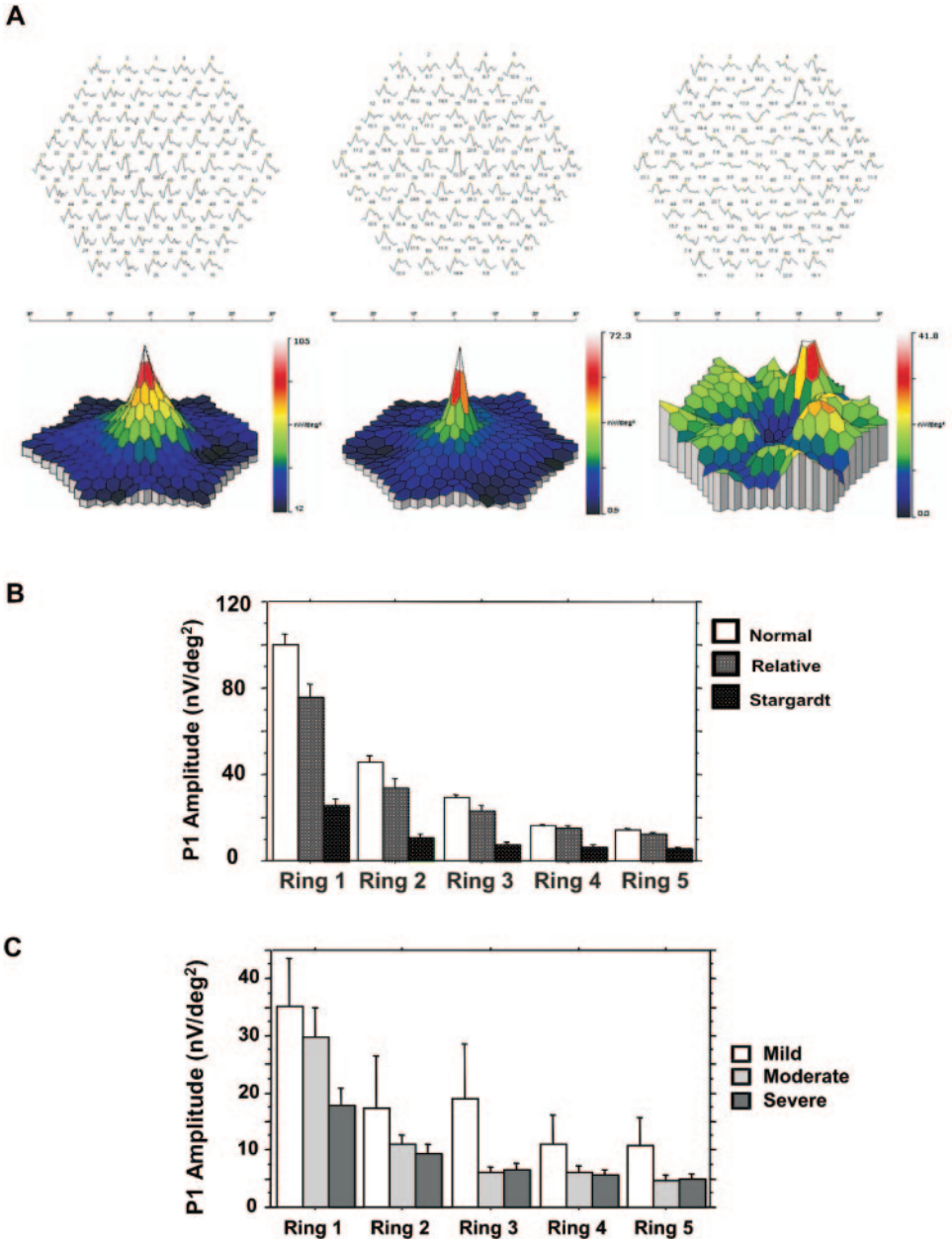

FIGURE 5. mfERG obtained from representative individuals of patients with STGD, STGD relatives, and control groups (**A**). Decreased mfERGs responses were observed in patients with STGD and relatives. (**B**) mfERG peak amplitudes for the P1 component were significantly reduced in different eccentricity rings up to 30°. (**C**) P1 amplitude responses across the different rings correlated highly with STGD disease stages (mild, moderate, and severe).

mfERG responses were globally correlated with psychophysical measures and were found to be dramatically impaired across the retina of patients with STGD. Our results corroborate previous work in STGD where functional defects were often not limited to the fovea and parafovea, but did affect peripheral retina more than expected by more conventional visual field measurements and ophthalmoscopy.[40]

Surprisingly, we found that morphologically nonaffected STGD relatives with normal VA were functionally impaired as revealed both psychophysical and electrophysiological approaches. Their visual performance, as measured by LSF and ISF tasks was between normal age-matched control subjects and patients with STGD.

Overall, 12 different mutations were identified in 80% of the asymptomatic STGD, including two new putative severe mutations (M1T, 4034delAC), which were segregated within the STGD families. The only proven wild-type homozygous relative (thereby serving as a negative control) was found to be at the 90th percentile for all phenotypical tasks.

A matter for future studies is a further investigation to determine the extent that the genetical profiles of impaired but morphologically unaffected relatives are related to the ones of overtly impaired STGD subjects and why in the former case are physiological alterations the sole manifestation of impairment. It is worth noting that mutations in *ABCA4* have a high prevalence in the general population (7%–8%)[41,42] Furthermore, previous studies have reported that residual ABCA4 activity correlates with the severity of the clinical phenotype, as reflected by the age of onset. Another interesting finding is that ABCA4 deficiency has been proved to cause or contribute to the manifestations of several other autosomal recessive retinal dystrophies—namely, cone–rod dystrophy, retinitis pigmentosa, and a apparent susceptibility to age-related macular degeneration (AMD), in both human and animal models.[16,17,43] Therefore, we suggest that apparently normal carriers, at least for some mutations, may have an insufficiency of *ABCA4* expression. This hypothesis is corroborated by recent work of Mata et al.,[43] and Wiszniewski et al.[44] who found that heterozy-

TABLE 2. Pathogenic Variants of the *ABCA4* Gene Found in Nonaffected Relatives

Family	Subjects	Phenotype	CFC	*ABCA4* Allele 1/Allele 2
1	ARP	No STGD (F)	No changes	N96D/wt
2	CAO	No STGD (S)	Subtle*	Wt/wt
3	GMB	No STGD (B)	No changes	IVS40+5G>A/wt
4	MAS	No STGD (S)	No changes	3211insGT/wt
5	MCA	No STGD (M)	No changes	M1V R2030Q/wt
6	LCB	No STGD (B)	No changes	R290W/wt
7	VCG	No STGD (S)	No changes	L2027F/wt
8	JMF	No STGD (B)	No changes	V2050L/wt
9	DRN	No STGD (M)	No changes	**M1T/** wt
10	SCR	No STGD (S)	No changes	G1961E/wt
11	AGK	No STGD (S)	No changes	L11P/wt
13	JLO	No STGD (B)	Subtle*	G1961E/wt
14	GBR	No STGD (F)	No changes	**4034delAC**/wt
18	CMD	No STGD (S)	No changes	Wt/wt
20	MLC	No STGD (M)	No changes	Wt/wt
21	BRG	No STGD (S)	No changes	ND

Family, nonaffected relative, phenotype, and relationship to the affected relative: F, father; M, mother; B, brother; S, sister, CFC, central fundus changes and *ABCA* mutations detected; wt, wild-type. Novel putative pathogenic variants are depicted in bold.

* Siblings CAO and JLO had subtle changes in their fundus but did not fulfill the criteria for Stargardt disease.

gous null mutations in the *ABCA* gene cause clinical signs that resemble STGD but with slower progression. Thus, we believe that relatives of persons with STGD should be followed-up, because their visual function as a group is subnormal. Given the similarity between STGD and AMD and that some high-prevalence mutations—namely, the variant G1961E—even in the heterozygous state, have been significantly associated with AMD, STGD carriers may well have some predisposition to the development of AMD, although this statement must at this point remain speculative. Moreover, some evidence for increased incidence of AMD in STGD families has been found.[45]

Future work on quantitative phenotyping and correlative mutation analysis of *ABCA4* in both patients with STGD and relatives may be promising to help predict early functional consequences of loss of ABCA4 activity that induces photoreceptor degeneration.

Acknowledgments

The authors thank the patients and their families for participating in the study and Ana Rita Vaz, Mário Soares, Pedro Melo, and Catarina Mateus for technical assistance.

References

1. Stargardt K. Über familäre, progressive Degeneration in der Maculagegend des Auges. *Graefes Arch Clin Exp Ophthalmol* 1909;71:534–550.
2. Kaplan J, Gerber S, Larget PD, et al. A gene for Stargardt's disease (fundus flavimaculatus) maps to the short arm of chromosome 1. *Nat Genet*. 1993;5:308–311.
3. Irvine AR, Wergeland FL Jr. Stargardt's hereditary progressive macular degeneration. *Br J Ophthalmol* 1972;56:817–826.
4. Blacharski PA. Fundus flavimaculatus. In: Newsom DA, ed. *Retinal Dystrophies and Degenerations*. New York: Raven Press; 1988; 135–159.
5. Noble KG, Carr RE. Stargardt's disease and fundus flavimaculatus. *Arch Ophthalmol*. 1979;97:1281–1285.
6. Aaberg TM. Stargardt's disease and fundus flavimaculatus: evaluation of morphologic progression and intrafamilial co-existence. *Trans Am Ophthalmol Soc*. 1986;84:453–487.
7. Armstrong JD, Meyer D, Shizhao X, Elfervig JL. Long-term follow-up of Stargardt's disease and fundus flavimaculatus. *Ophthalmology*. 1998;105:448–458.
8. Lois N, Holder GE, Fitzke FW, Plant C, Bird AC. Intrafamilial variation of phenotype in Stargardt macular dystrophy-fundus flavimaculatus. *Invest Ophthalmol Vis Sci*. 1999;40:2668–2675.
9. Fishman GA. Fundus flavimaculatus. *Arch Ophthalmol*. 1976;94:2061–2067.
10. Delori FC, Staurenghi G, Arend O, Dorey CK, Goger DG, Weiter JJ. In vivo measurement of lipofuscin in Stargardt's disease-fundus flavimaculatus. *Invest Ophthalmol Vis Sci*. 1995;36:2327–2331.
11. Fishman GA, Stone EM, Grover S, Derlacki DJ, Haines HL, Hockey RR. Variation of clinical expression in patients with Stargardt dystrophy and sequence variations in the ABCR gene. *Arch Ophthalmol* 1999;117:504–510.
12. Allikmets R, Singh N, Sun H, et al. A photoreceptor cell-specific ATP-binding transporter gene (ABCR) is mutated in recessive Stargardt macular dystrophy. *Nat Genet*. 1997;15:236–246.
13. Webster AR, Heon E, Lotery AJ, et al. An analysis of allelic variation in the *ABCA4* gene. *Invest Ophthalmol Vis Sci*. 2001;42:1179–1189.
14. Shroyer NF, Lewis RA, Lupski JR. Complex inheritance of ABCR mutations in Stargardt disease: linkage disequilibrium, complex alleles, and pseudodominance. *Hum Genet*. 2000;106:244–248.
15. Rivera A, White K, Stohr H, et al. A comprehensive survey of sequence variation in the ABCA4 (ABCR) gene in Stargardt disease and age-related macular degeneration. *Am J Hum Genet*. 2000;67:800–813.
16. Allikmets R, Shroyer NF, Singh N, et al. Mutation of the Stargardt disease gene (ABCR) in age-related macular degeneration. *Science*. 1997;277:1805–1807.
17. Martinez-Mir A, Paloma E, Allikmets R, et al. Retinitis pigmentosa caused by a homozygous mutation in the Stargardt disease gene ABCR. *Nat Genet*. 1998;18:11–12.
18. van Driel MA, Maugeri A, Klevering BJ, Hoyng CB, Cremers FP ABCR unites what ophthalmologists divide(s). *Ophthalmic Genet.* 1998;19:117–122.
19. Sun H, Nathans J. Stargardt's ABCR is localized to the disc membrane of retinal rod outer segments. *Nat Genet* 1997;17:15–16.
20. Molday LL, Rabin AR, Molday RS. ABCR expression in foveal cone photoreceptors and its role in Stargardt macular dystrophy. *Nat Genet*. 2000;25:257–258.
21. Scholl HPN, Kremers J, Vonthein R, White K, Weber BH. L- and M-cone driven electroretinograms in Stargardt's macular dystrophy-fundus flavimaculatus. *Invest Ophthalmol Vis Sci* 2001;42:1380–1389.

22. Campos SH, Forjaz V, Kozak LR, Silva E, Castelo-Branco M. Quantitative phenotyping of chromatic dysfunction in Best macular dystrophy. *Arch Ophthalmol*. 2005;123:944–949.
23. Castelo-Branco M, Faria P, Forjaz V, Kozak LR, Azevedo H. Early and late damage of parvo- and koniocellular function in ocular hypertension and glaucoma. *Invest Ophthalmol Vis Sci* 2005;45 (2):499–505.
24. Wyszecki G, Stiles WS. *Color Science: Concepts and Methods*: *Quantitative Data.* 2nd ed. New York: John Wiley & Son; 1982.
25. Silva MF, Faria P, Regateiro FS, et al. Independent patterns of damage within magno-, parvo- and koniocellular pathways in Parkinson's disease. *Brain* 2005;128:2260–2271.
26. Mendes M, Silva F, Simoes L, Jorge M, Saraiva J, Castelo-Branco M. Visual magnocellular and structure from motion perceptual deficits in a neurodevelopmental model of dorsal stream function. *Brain Res Cogn Brain Res*. 2005;25 (3):788–798.
27. Caprioli J. Automated perimetry in glaucoma. *Am J Ophthalmol*. 1991;111:235–239.
28. Hood DC, Seiple W, Holopigian K, Greenstein V. A comparison of the components of the multifocal and full-field ERGs. *Vis Neurosci*. 1997;14:533–544.
29. Jaakson K, Zernant J, Kulm M. et al. Genotyping microarray (gene chip) for the ABCR (ABCA4) gene. *Hum Mutat*. 2003;22:395–403.
30. Simonelli F, Testa F, de Crecchio G, et al. New ABCR mutations and clinical phenotype in Italian patients with Stargardt disease. *Invest Ophthalmol Vis Sci* 2000;41:892–897.
31. Boon CJ, van Schooneveld MJ, den Hollander AI, et al. Mutations in the peripherin/RDS gene are an important cause of multifocal pattern dystrophy simulating STGD1/fundus flavimaculatus. *Br J Ophthalmol* 2007;91:1504–1511.
32. Alexander KR, Barnes CS, Fishman GA, Pokorny J, Smith VC. Contrast sensitivity deficits in inferred magnocellular and parvocellular pathways in retinitis pigmentosa. *Invest Ophthalmol Vis Sci*. 2004;45:4510–4519.
33. Alexander KR, Rajagopalan AS, Seiple W, Zemon VM, Fishman GA. Contrast response properties of magnocellular and parvocellular pathways in retinitis pigmentosa assessed by the visual evoked potential. *Invest Ophthalmol Vis Sci*. 2005;46:2967–2973.
34. Silveira LC, Yamada ES, Perry VH, Picanco-Diniz CW. M and P retinal ganglion cells of diurnal and nocturnal New-World monkeys. *Neuroreport*. 1994;5:2077–2081.
35. Merigan WH, Maunsell JH. How parallel are the primate visual pathways? *Annu Rev Neurosci*. 1993;16:369–402.
36. Dandona L, Hendrickson A, Quigley HA. Selective effects of experimental glaucoma on axonal transport by retinal ganglion cells to the dorsal lateral geniculate nucleus. *Invest Ophthalmol Vis Sci*. 1991;32:1593–1599.
37. Maddess T, Goldberg I, Wine S, Dobinson J, Welsh AH, James AC. Testing for glaucoma with the spatial frequency doubling illusion. *Vision Res*. 1999;39:4258–4273.
38. Perry VH, Cowey A. The ganglion cell and cone distribution in the monkey retina: implications for central magnification factors. *Vision Res*. 1985;25:1795–1810.
39. Yamada ES, Silveira LC, Perry VH, Franco EC. M and P retinal ganglion cells of the owl monkey: morphology, size and photoreceptor convergence. *Vision Res*. 2001;41:119–131.
40. Kretschmann U, Seeliger MW, Ruether K, Usui T, Apfelstedt-Sylla E, Zrenner E. Multifocal electroretinography in patients with Stargardt's macular dystrophy. *Br J Ophthalmol* 1998;82:267–275.
41. Maugeri A, van Driel MA, van de Pol, et al. The 2588G→C mutation in the ABCR gene is a mild frequent founder mutation in the Western European population and allows the classification of ABCR mutations in patients with Stargardt disease. *Am J Hum Genet.* 1999;64:1024–1035.
42. Maugeri A, Flothmann K, Hemmrich N, et al. The ABCA4 2588G.C Stargardt mutation: single origin and increasing frequency from South-West to North-East Europe. *Eur J Hum Genet.* 2002;10:197–203.
43. Mata NL, Tzekov RT, Liu X, Weng J, Birch DG, Travis GH. Delayed dark-adaptation and lipofuscin accumulation in abcrþ/2 mice: implications for involvement of ABCR in age-related macular degeneration. *Invest Ophthalmol Vis Sci.* 2001;42,1685–1690.
44. Wiszniewski W, Zaremba C, Yatsenko A, et al. ABCA4 mutations causing mislocalization are found frequently in patients with severe retinal dystrophies. *Hum Mol Genet*. 2005;14(19):2769–2778.
45. Souied EH, Ducroq D, Gerber S, et al. Age-related macular degeneration in grandparents of patients with Stargardt disease: genetic study. *Am J Ophthalmo*l. 1999;128(2):173–178.